International Journal of Mass Spectrometry 306 (2011) 44–50

Contents lists available at ScienceDirect

International Journal of Mass Spectrometry

journal homepage: www.elsevier.com/locate/ijms

Temperature dependence of magic number and first hydrated shell of various core water cluster ions $Y^-(H_2O)_n$ ($Y = O_2$, HO_x, NO_x, CO_x) in atmospheric pressure negative corona discharge mass spectrometry

Kanako Sekimoto [a], Kei Kikuchi [b], Mitsuo Takayama [b,*]

[a] Atmospheric Environment Division, National Institute for Environmental Studies, 16-2 Onogawa, Tsukuba, Ibaraki 305-8506, Japan
[b] Graduate School of Nanobioscience, Yokohama City University, 22-2 Seto, Kanazawa-ku, Yokohama, Kanagawa 236-0027, Japan

ARTICLE INFO

Article history:
Received 26 January 2011
Received in revised form 13 June 2011
Accepted 13 June 2011
Available online 21 June 2011

Keywords:
Negative corona discharge
Water cluster
Atmospheric chemistry
Magic number
First hydrated shell

ABSTRACT

The relationship between orifice temperature and the size distribution in water clusters $Y^-(H_2O)_n$ with various negative atmospheric core ions Y^- such as O_2^-, HO^-, HO_2^-, NO_2^-, NO_3^-, $NO_3^-(HNO_3)_2$, CO_3^- and HCO_4^- has been investigated using atmospheric pressure negative corona discharge mass spectrometry. Although the cluster distributions shifted in the lower-mass region with increasing orifice temperature due to insufficient cooling during adiabatic expansion, the anomalous discontinuities in ion peak intensity at certain size clusters $Y^-(H_2O)_m$ in the $Y^-(H_2O)_n$ cluster series reproducibly observed at the lowest orifice temperature did not vary with change in temperature. The results obtained suggest that the clusters $Y^-(H_2O)_m$ have particular thermochemical stability compared to other size clusters $Y^-(H_2O)_n$ under arbitrary temperature conditions, and that the $Y^-(H_2O)_m$ would correspond to the magic number or first hydrated shell in the cluster series $Y^-(H_2O)_n$. The specific stability of $Y^-(H_2O)_m$ was also confirmed by using the ratio of $Y^-(H_2O)_n$ to $Y^-(H_2O)_{n+1}$ peak intensity, which is a reliable method to identify the magic numbers in arbitrary cluster distributions obtained by varying the temperature and solvent partial pressure in a reaction chamber.

1. Introduction

Atmospheric ion water clusters, e.g., $H_3O^+(H_2O)_n$, $O_2^-(H_2O)_n$ and $NO_x^-(H_2O)_n$, have been of long-standing interest in the field of atmospheric sciences, because of their central role in the formation of tropospheric aerosols which affect photochemistry, radiation budget of the atmosphere and climate. On the basis of a mechanism of aerosol formation in the troposphere proposed by Yu and Turco, termed "ion-mediated nucleation" [1], atmospheric ion water clusters are most likely to be produced *via* three processes;

(1) atmospheric core ion formation by evolution of primary ions such as $N_2^{\bullet+}$, $O_2^{\bullet+}$, O^- and O_2^- through successive ion–molecule reactions with air constituents,
(2) generation of ion-induced water clusters by direct attachment of polar solvent molecules (H_2O) to atmospheric core ions due to them having strong binding energy *via* ion–dipole interactions, and
(3) growth of ion-induced hydrates into large water clusters bound *via* hydrogen-bonding networks by condensation with H_2O molecules.

Specific water cluster ions having significant thermochemical stability, i.e., the first hydrated shells and magic numbers which have the first hydration shell filled and symmetrical clathrate structures, respectively, occur in the formation process of water clusters. Those particularly stable clusters serve as nuclei for the growth of water clusters into tropospheric aerosols. Knowledge of the first hydrated shells and magic numbers for individual atmospheric core ions, therefore, would contribute toward further understanding of the formation mechanism of tropospheric aerosols.

Mass spectrometry analysis is a powerful tool for thermochemical studies of water cluster systems in the gas phase. The water cluster distributions observed in mass spectra and the van't Hoff plot based on cluster ion peak intensities provide the information about the first hydrated shell and magic numbers in a series of water cluster ions. A large number of mass spectra of well-known positive atmospheric ion water clusters $H_3O^+(H_2O)_n$ have been obtained using various experimental conditions such as field emission ionization in water vapor [2,3], free jet expansion of water vapor with electron impact [4,5], liquid ionization [6], electrospray [7], discharge ionization [8,9], ion bombardment of ice

* Corresponding author. Tel.: +81 45 787 2431.
E-mail address: Takayama@yokohama-cu.ac.jp (M. Takayama).

1387-3806/$ – see front matter © 2011 Elsevier B.V. All rights reserved.
doi:10.1016/j.ijms.2011.06.007

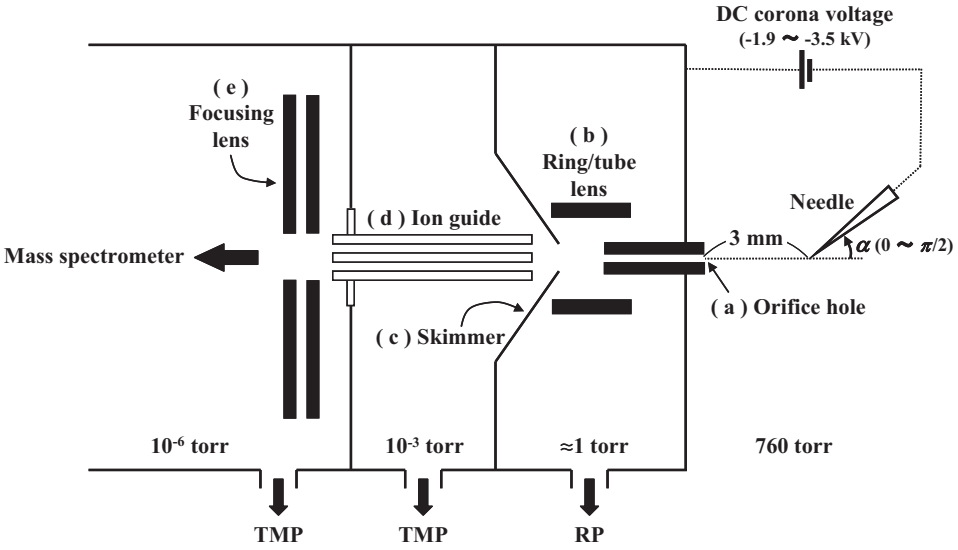

Fig. 1. Schematic illustration of the atmospheric pressure corona discharge mass spectrometer used in the present study.

surfaces [10] and vapor threshold vacuum-UV photoionization of neutral clusters [11]. These were performed at temperatures over the range of 120–350 K. All the mass spectra obtained exhibited anomalous discontinuities in ion peak intensity at $H_3O^+(H_2O)_3$, $H_3O^+(H_2O)_{20}$ and $H_3O^+(H_2O)_{27}$, independent of the ionization methods and temperature conditions in reaction chambers. Kinetic studies have exhibited a discontinuous gap in the van't Hoff plot for $H_3O^+(H_2O)_n$ (n = 0–6) between n = 3 and 4 [12–14]. These facts indicate that $H_3O^+(H_2O)_3$, and $H_3O^+(H_2O)_{20}$ and $H_3O^+(H_2O)_{27}$ correspond to the first hydrated shell and magic numbers in the $H_3O^+(H_2O)_n$ cluster series, respectively. *Ab initio* molecular orbital calculations have reported that $H_3O^+(H_3O)_3$ has a C_3 arrangement with three H_2O molecules surrounding the core H_3O^+ ion, while $H_3O^+(H_2O)_{20}$ and $H_3O^+(H_2O)_{27}$ have a clathrate structure with 20 oxygen atoms forming a dodecahedron with D symmetry surrounding the central cavity that contains an additional H_2O molecule or core H_3O^+ ion and 16-hedral structure, respectively [8,9,11,15–17]. In contrast, there is little thermochemical information for negative atmospheric ion water clusters. This absence of information is due to the lack of experimental methods for the reproducible formation of the specific negative core ions and their hydrates and the resulting difficulties in obtaining reliable mass spectrometry data from negative ion water clusters.

We have recently reported reliable mass spectrometry data for large water clusters $Y^-(H_2O)_n$ with various negative core ions Y^- which play a central role in tropospheric ion chemistry, i.e., O_2^-, HO^-, HO_2^-, NO_2^-, NO_3^-, $NO_3^-(HNO_3)_2$, CO_3^- and HCO_4^-, by using atmospheric pressure DC negative corona discharge mass spectrometry [18]. An atmospheric pressure DC corona discharge device containing a specific corona needle made it possible to reproducibly generate various negative core ions Y^- originating from ambient air [19–21]. Furthermore, the use of the discharge system coupled with mass spectrometers led to the stable formation of large water clusters $Y^-(H_2O)_n$ due to adiabatic expansion caused by the pressure difference between the ambient discharge area (760 Torr) and vacuum region in the mass spectrometers (≈1 Torr). The mass spectra of individual negative ion water clusters reported showed reproducible discontinuities in the ion peak intensity at certain size clusters $Y^-(H_2O)_m$, which indicates that specific clusters have particular thermochemical stability in the cluster series $Y^-(H_2O)_n$ [18]. Thus, the $Y^-(H_2O)_m$ may correspond to the magic number or first hydrated shell for the $Y^-(H_2O)_n$. The high intensity discontinuity at $HO^-(H_2O)_3$ observed in the mass spectrum of $HO^-(H_2O)_n$ was the first direct mass spectrometric evidence for specific stability of $HO^-(H_2O)_3$ as the first hydrated shell in the $HO^-(H_2O)_n$ cluster series which Eigen postulated [17].

It is already known that various size distributions in water clusters obtained by changing the experimental conditions, temperature and water vapor partial pressure in a reaction chamber, are useful to estimate the specific water clusters with particular thermochemical stability [22]. In order to confirm the particular stability of the $Y^-(H_2O)_m$ in the cluster series $Y^-(H_2O)_n$ recently reported, here we investigate the change in intensity of the $Y^-(H_2O)_m$ ion peaks in various size distributions of $Y^-(H_2O)_n$ obtained by varying orifice temperature which influences the adiabatic expansion effect for the growth of water clusters. The results obtained here provide experimental evidence for the first hydrated shell and magic numbers in a series of various negative atmospheric ion water clusters.

2. Experimental

2.1. Atmospheric pressure DC negative corona discharge mass spectrometry

Discharge experiments using point-to-plane electrodes were performed under atmospheric pressure in room air without any preparation. The laboratory temperature (298 K) and relative humidity (50–70%) were controlled by an air-conditioner. The corona needle used as the point electrode was a headless stainless steel pin (Shiga, Tokyo, Japan) with a diameter of 200 μm and 20 mm in length. The needle tip had a radius of curvature of ca. 1 μm and the shape of the tip surface was adequately approximated by a hyperboloid of revolution. The opposite electrode was the orifice plate of a mass spectrometer made of stainless steel. The discharge gap between the electrodes and needle angle α with respect to the orifice hole axis were adjusted 3 mm and over the range of 0–π/2 rad, respectively, using a manipulator (see Fig. 1). An angle of 0 means that the needle was located on the orifice hole axis. DC voltages over the range of −1.9 to −3.5 kV were applied to the needle relative to the orifice plate in order to establish a stationary electric field between the electrodes. The corona voltages used led to stable glow corona on the needle tip and brought about electric current over the range of 3.3–40 μA which was measured with a micro-ammeter.

Table 1
Discharge conditions, mass spectrometers used and resulting negative core ion species.

	Double-focusing mass spectrometer	Triple-quadrupole mass spectrometer
(a) Orifice hole		
Inner diameter (μm)	130	320
Length (mm)	5	114
Temperature (K)	308–383	333–373
Applied DC voltage (V)	0	20
(b) Ring/tube lens		
Applied DC voltage (V)	50	67.8
(c) Skimmer		
Applied DC voltage (V)	25	0
(d) Ion guide		
Applied RF voltage (V)	2.6	3
(e) Focusing lens		
Applied DC voltage (V)	2500	20.5

Mass spectra were acquired on a JMS-LCmate reversed geometry double-focusing mass spectrometer (JEOL, Tokyo, Japan) and a TSQ7000 triple-quadrupole mass spectrometer (Thermo Fisher Scientific, San Jose, CA). Both mass spectrometers consisted of three parts; the first differential pumping region between an orifice exit and skimmer which was maintained at ca. 1 Torr, the second differential pumping region including an ion guide at 10^{-3} Torr, and an analyzer at 10^{-6} Torr. Fig. 1 shows a schematic illustration of the experimental apparatus used. The two types of mass spectrometers differed from one another in configuration of the orifice hole and the first differential pumping region and range of the orifice hole temperature which led to stable distribution mass spectra consisting of water cluster ions $Y^-(H_2O)_n$. The inner diameter, length and temperature of the orifice hole and voltages applied on the orifice hole, ring/tube lens, skimmer, ion guide, and focusing lens for ion acceleration for each mass spectrometer are listed in Table 1. The mass spectra of the negative ion water clusters $Y^-(H_2O)_n$ obtained at the lowest orifice temperatures of individual mass spectrometers have been reported elsewhere [18]. The relative peak intensity $RI(Y^-(H_2O)_i)$ (%) of a certain size water cluster $Y^-(H_2O)_i$ ($i \geq 0$) in the $Y^-(H_2O)_n$ cluster series was calculated from the measured absolute peak intensity $I(Y^-(H_2O)_i)$ (arbitrary unit), which is proportional to the number of detected ions, by the following equation:

$$RI(Y^-(H_2O)_i)(\%) = \frac{I(Y^-(H_2O)_i)}{\sum I(Y^-(H_2O)_i)} \times 100$$

2.2. Formation of water clusters with various negative atmospheric core ions

The detailed mechanism for the formation of large water clusters $Y^-(H_2O)_n$ with negative core ions Y^- such as O_2^-, HO^-, HO_2^-, NO_2^-, NO_3^-, $NO_3^-(HNO_3)_2$, CO_3^-, and HCO_4^- by atmospheric pressure DC negative corona discharge mass spectrometry can be found elsewhere [18] and is only briefly described here. The negative ion water clusters $Y^-(H_2O)_n$ observed in the experimental system used here are most likely produced *via* three processes; (1) core ion formation *via* ion evolution, (2) subsequent generation of ion-induced water clusters in the ambient discharge area (760 Torr) and/or inside of the orifice hole (≈760 Torr), and (3) growth of water clusters by adiabatic expansion in the vacuum region (≈1 Torr). The use of the specific discharge conditions with respect to corona voltage V and needle angle α and mass spectrometers with different orifice hole lengths resulted in the dominant generation of various different negative core ions Y^- described above. The discharge conditions (V, α), mass spectrometers used and resulting core ions are summarized in Table 2. Core ion formation is strongly dependent on the electric field strength on the needle tip surface determined by the corona voltage and needle angle. The low field strength originating from low voltage (<2.5 kV) and large angle ($\pi/2$) brings about the dominant formation of the core ions O_2^- and HO_x^- with short lifetimes in air ($\leq 10^{-3}$ s), while the longer-lived core ions NO_x^- and CO_x^- ($\geq$1 s) are mainly produced at high field strength attributed to high voltage (>2.5 kV) and small angle ($<\pi/2$). Furthermore, the change in ion evolution time depending on the orifice hole length brings about the production of different core ion species even when using the same discharge conditions, e.g., $(V, \alpha) = (-3.5, 0)$ and $(-1.9, \pi/2)$ in Table 2.

3. Results and discussion

3.1. Dependence of water cluster distribution on orifice temperature

Figs. 2 and 3 show the relative peak intensities of various negative ion water clusters $Y^-(H_2O)_n$ for several orifice temperatures as a function of cluster size n, obtained using the double-focusing and triple-quadrupole mass spectrometers, respectively. The core ions Y^- shown in Fig. 2 are (a) HO^-, (b) HO_2^-, (c) NO_2^-, and (d) NO_3^-. In the case of the water cluster series shown in Fig. 3 they are (a) O_2^-, (b) CO_3^-, (c) HCO_4^-, and (d) $NO_3^-(HNO_3)_2$. The distributions of water clusters with high peak intensity were shifted to smaller cluster size with increasing orifice temperature, as shown in Figs. 2 and 3. According to the formation mechanism of the negative ion water clusters in our experimental system previously reported [18], the core ions Y^- and ion-induced water clusters $Y^-(H_2O)_l$ including the first hydrated shell $Y^-(H_2O)_{l^*}$ ($l < l^*$) are produced in the ambient discharge area (760 Torr) and/or inside of the orifice hole (≈760 Torr). In contrast, large water clusters $Y^-(H_2O)_n$ ($n > l^*$) form due to adiabatic expansion occurring in the first differential pumping regions of the mass spectrometer (≈1 Torr). The increase in orifice temperature brings about an increase in temperature of background gases in the vacuum regions of the mass spectrometer, resulting in inefficient adiabatic cooling of supersonic expansion. It is most likely, therefore, that the shift to smaller cluster size with increasing orifice temperature observed here can be attributed to the inhibition of large water cluster formation due to inefficient adiabatic expansion.

It was mentioned in our previous report that the mass spectra of large water clusters $Y^-(H_2O)_n$ with individual negative core ions Y^- obtained at the lowest orifice temperatures exhibited reproducible anomalous discontinuities in the peak intensity at certain size clusters $Y^-(H_2O)_m$ [18]. The cluster size m for each core ion Y^- previously reported is represented in italic numbers in Figs. 2 and 3. It should be noted in those figures that the intensity discontinuities in the cluster size m did not vary with change in temperature, although the cluster distributions shifted. These results suggest that the clusters $Y^-(H_2O)_m$ have particular thermochemical stability compared to other size clusters $Y^-(H_2O)_n$, independent of temperature conditions. It is most likely, therefore, that the clusters $Y^-(H_2O)_m$ with intensity discontinuity under arbitrary orifice temperatures shown in Figs. 2 and 3 correspond to the magic number or first hydrated shell in the $Y^-(H_2O)_n$ cluster series.

3.2. Peak intensity ratio of water clusters

The stability of $Y^-(H_2O)_n$ was investigated using the ratio of $Y^-(H_2O)_n$ to $Y^-(H_2O)_{n+1}$ peak intensity ($R = RI(Y^-(H_2O)_n)/RI(Y^-(H_2O)_{n+1})$, which was proposed by Zhang et al. as a reliable method for identifying the magic numbers in arbitrary cluster distributions obtained by varying the temperature and solvent partial pressure in a reaction chamber [8]. The intensity ratio R evaluated from Figs. 2 and 3 is replotted as a

Table 2
The conditions used in the two different mass spectrometers employed in this study.

Double-focusing mass spectrometer (orifice hole length, 5 mm)		Triple-quadrupole mass spectrometer (orifice hole length, 114 mm)	
Core ion species	Discharge condition (V (kV), α (rad))	Core ion species	Discharge condition (V (kV), α (rad))
NO_3^-	(−3.5, 0)	$NO_3^-(HNO_3)_2$	(−3.5, 0)
NO_2^-	(−2.5, 0)	HCO_4^-	(−3.1, π/4)
HO_2^-	(−2.5, π/4)	CO_3^-	(−2.7, π/4)
HO^-	(−1.9, π/2)	O_2^-	(−1.9, π/2)

function of cluster size n in Figs. 4 and 5. Figs. 4 and 5 indicate that the intensity ratio is not very sensitive to the temperature conditions, while the original cluster distributions are considerably changed with varying temperature (see Figs. 2 and 3). It should be noted in Figs. 4 and 5 that distinct peaks in the intensity ratio at all the clusters $Y^-(H_2O)_m$ except for $HO^-(H_2O)_3$ in Fig. 4a and $NO_3^-(H_2O)_2$ in Fig. 4d, which are represented by black arrow marks in Figs. 4 and 5, were clearly seen at all temperature conditions. These predominant peaks are similar to those for the positive ion magic number $H_3O^+(H_2O)_{20}$ observed under different temperature conditions (123 and 135 K) in a flow tube reactor which has been reported by Zhang et al. [8]. These results therefore suggest that the clusters $Y^-(H_2O)_m$ with distinct peaks in intensity ratio are particularly stable compared to other size clusters $Y^-(H_2O)_n$ under arbitrary temperature conditions, and hence, those clusters correspond to the magic numbers for the $Y^-(H_2O)_n$ cluster series.

In contrast, the peak intensity ratio patterns in the neighborhood of $HO^-(H_2O)_3$ and $NO_3^-(H_2O)_2$ which are the clusters $Y^-(H_2O)_m$ that were not observed as distinct peaks in intensity ratio have common features. That is, the peak intensity ratio at $Y^-(H_2O)_{m+1}$ ($HO^-(H_2O)_4$ and $NO_3^-(H_2O)_3$ in this case) is significantly lower than that for $Y^-(H_2O)_m$ and $Y^-(H_2O)_{m+2}$ at all the orifice temperatures as shown in Fig. 4a and d, indicating that the clusters $Y^-(H_2O)_{m+1}$ are unstable compared to $Y^-(H_2O)_m$ and $Y^-(H_2O)_{m+2}$ under arbitrary temperature conditions. The cluster $HO^-(H_2O)_3$ has been reported as the first hydrated shell in the $HO^-(H_2O)_n$ cluster series, by the Eigen postulation [17] and several methods such as use of the van't Hoff plot for $HO^-(H_2O)_n$ (n = 0–7) [14,23], high resolution vibrational spectroscopy of $HO^-(H_2O)_n$ (n = 1–5) [24], *ab initio* calculations of ΔH° and ΔG° for $HO^-(H_2O)_n$ (n = 1–4) [16], and similar calculations for the structure of $HO^-(H_2O)_3$ [16,24,25]. It is most likely, therefore, that attachment energies after the addition of the 4th H_2O molecule to form the secondary hydrated shell $HO^-(H_2O)_n$ ($n \geq 4$) are substantially smaller than those up to the 3rd H_2O for building the first hydrated shell $HO^-(H_2O)_3$. The discontinuous drop in attachment energy at the 4th H_2O molecule can lead to the specific unstable structure of $HO^-(H_2O)_4$, and result in an anomalous low intensity ratio at $HO^-(H_2O)_4$ as shown in Fig. 4a. It should be noted in Figs. 4 and 5 that the peak intensity ratio patterns observed not only at $NO_3^-(H_2O)_2$ but also at $O_2^-(H_2O)_4$, $CO_3^-(H_2O)_2$ and $HCO_4^-(H_2O)_3$ (represented by white arrow marks in Figs. 4 and 5) are in good agreement with that observed at $HO^-(H_2O)_3$. These findings suggest that $NO_3^-(H_2O)_2$, $O_2^-(H_2O)_4$, $CO_3^-(H_2O)_2$ and $HCO_4^-(H_2O)_3$ are the first hydrated shells for individual core water cluster ions $Y^-(H_2O)_n$ (Y = NO_3, O_2, CO_3 and HCO_4). Certainly, the specific high stability of $O_2^-(H_2O)_4$, $CO_3^-(H_2O)_2$ and $HCO_4^-(H_2O)_3$ can be directly observed as anomalous intensity discontinuities in the mass spectra obtained at higher

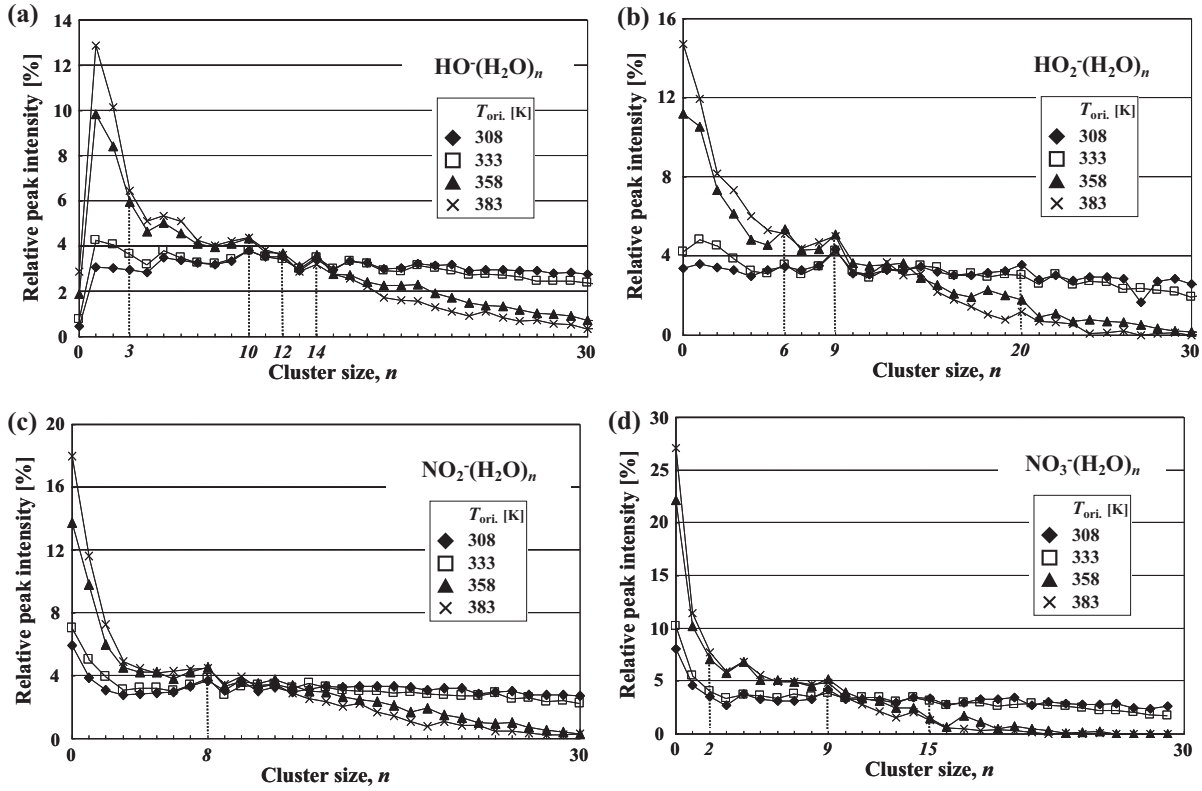

Fig. 2. Relative peak intensity of the negative ion water clusters $Y^-(H_2O)_n$ for several orifice temperatures as a function of cluster size n, obtained by using the double-focusing mass spectrometer. The core ion Y^- in each figure is (a) HO^-, (b) HO_2^-, (c) NO_2^-, and (d) NO_3^-.

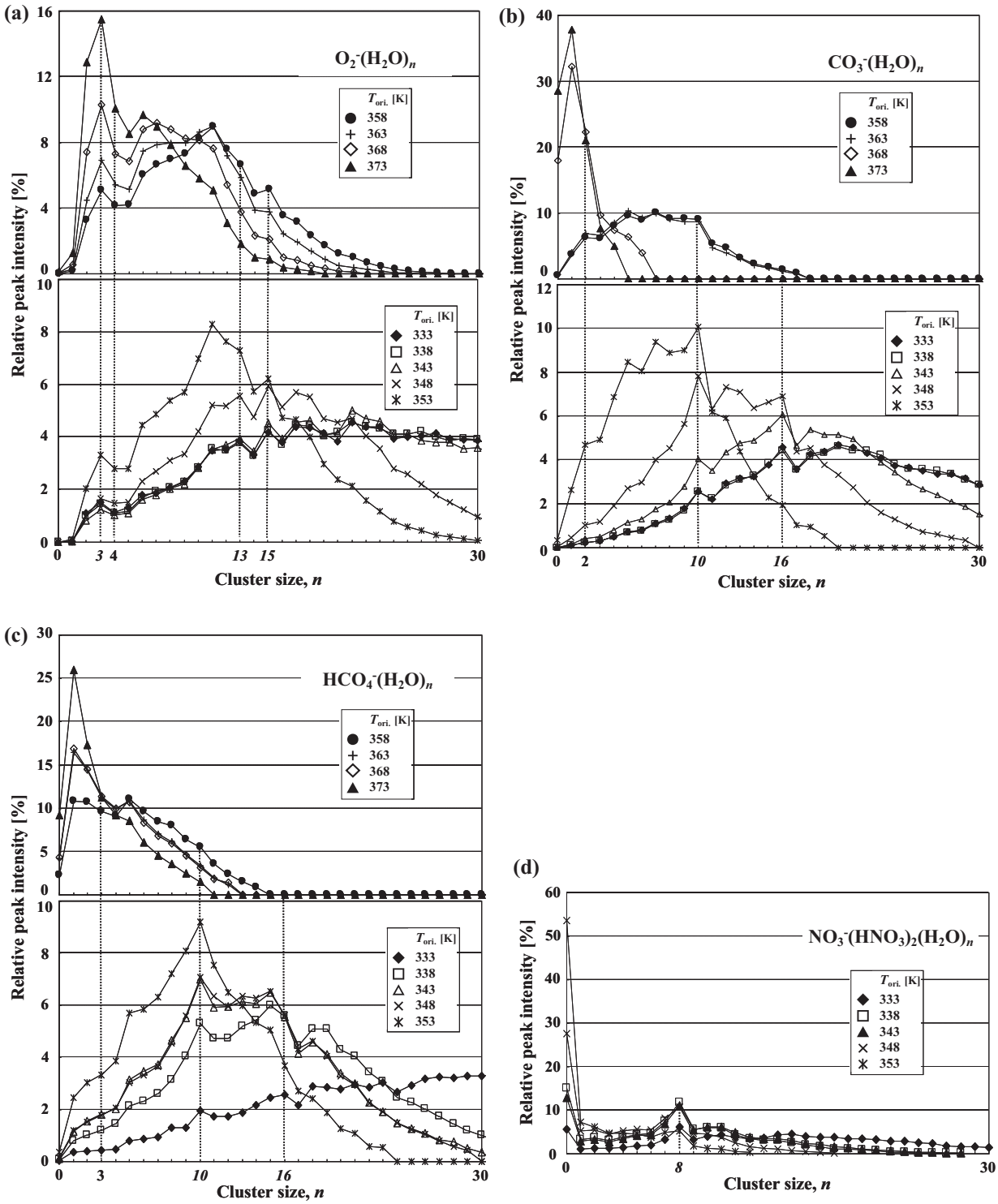

Fig. 3. Relative peak intensity of the negative ion water clusters $Y^-(H_2O)_n$ for several orifice temperatures as a function of cluster size n, obtained by using the triple-quadrupole mass spectrometer. The core ion Y^- in each figure is (a) O_2^-, (b) CO_3^-, (c) HCO_4^-, and (d) $NO_3^-(HNO_3)_2$.

orifice temperatures (upper in Fig. 3a–c). The cluster size of the magic numbers and first hydrated shell for various core water cluster ions $Y^-(H_2O)_n$ estimated in the present study are summarized in Table 3.

An interesting result of the present study is the finding of the specific high stability of $O_2^-(H_2O)_3$ and $O_2^-(H_2O)_4$ in the $O_2^-(H_2O)_n$ cluster series. The observation of the stability of $O_2^-(H_2O)_4$ as the first hydrated shell is in good agreement with previous studies [26–28]. Weber et al. reported the requirement for four H_2O molecules to complete the coordinate shell of the superoxide O_2^-, using infrared spectra of size-selected $O_2^-(H_2O)_n$ (n = 1–5) cluster ions obtained by photo-evaporation of an argon nano-matrix and *ab initio* calculations for stable structures of $O_2^-(H_2O)_4$ [26,27]. The $O_2^-(H_2O)_4{\cdot}Ar_3$ spectrum and the theoretical results revealed a structure in which each H_2O molecule is engaged in a single hydrogen bond to one of the four lobes of the π^* orbital of O_2^-, whereas the H_2O molecules bind together as pairs. Seta et al. calculated the structures of the first hydrated shells

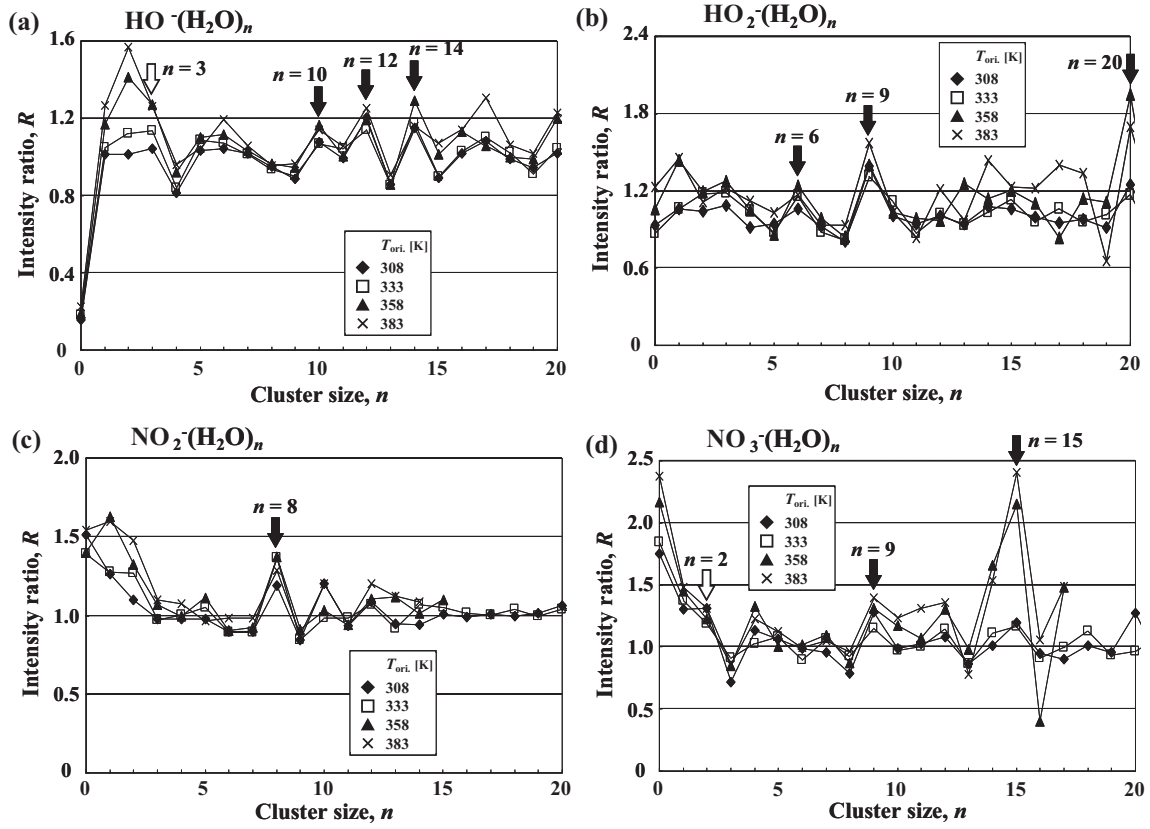

Fig. 4. The ratio of $Y^-(H_2O)_n$ to $Y^-(H_2O)_{n+1}$ peak intensity ($R = RI(Y^-(H_2O)_n)/RI(Y^-(H_2O)_{n+1})$ evaluated by Fig. 1. The core ion Y^- in each figure is (a) HO^-, (b) HO_2^-, (c) NO_2^-, and (d) NO_3^-. Black and white arrow marks represent the cluster size of magic number and first hydrated shell for individual core water cluster ions $Y^-(H_2O)_n$, respectively.

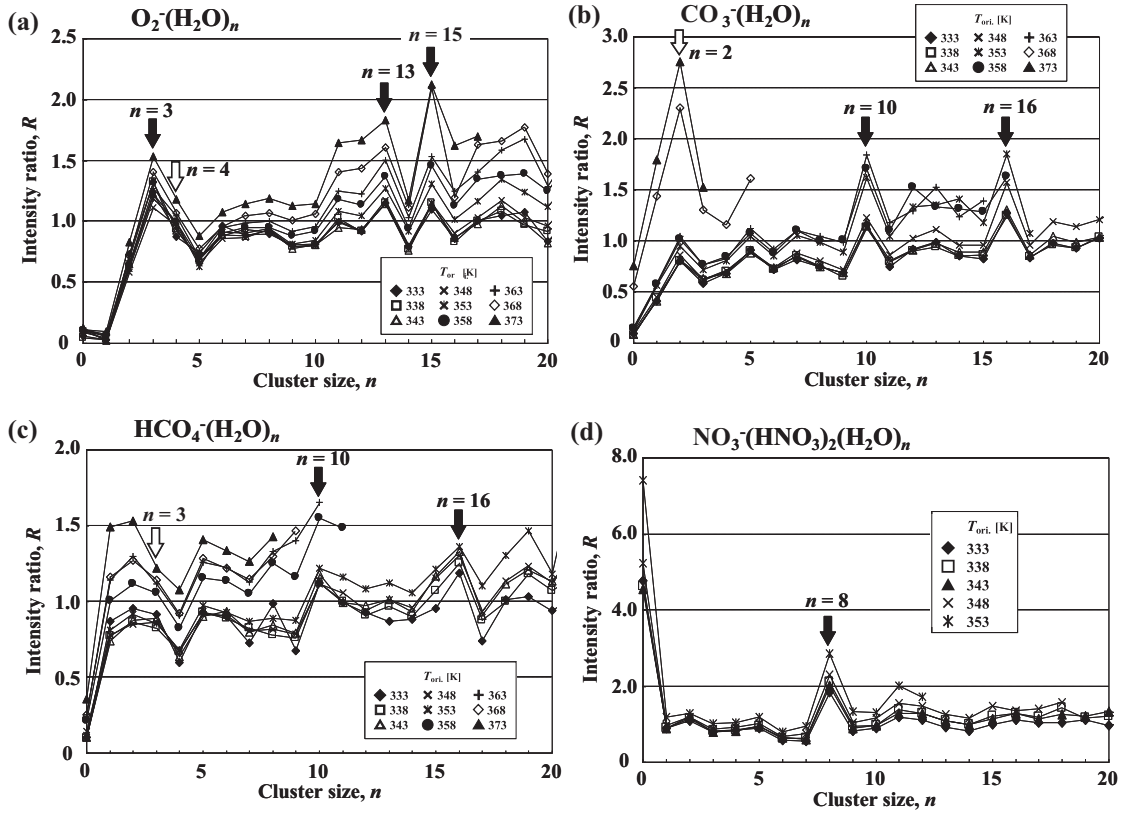

Fig. 5. The ratio of $Y^-(H_2O)_n$ to $Y^-(H_2O)_{n+1}$ peak intensity ($R = RI(Y^-(H_2O)_n)/RI(Y^-(H_2O)_{n+1})$ evaluated in Fig. 2. The core ion Y^- in each figure is (a) O_2^-, (b) CO_3^-, (c) HCO_4^-, and (d) $NO_3^-(HNO_3)_2$. Black and white arrow marks represent the cluster size of magic number and first hydrated shell for individual core water cluster ions $Y^-(H_2O)_n$, respectively.

Table 3
Cluster size of magic number and first hydrated shell for various core water cluster ions $Y^-(H_2O)_n$ estimated in the present study.

Core ion species, Y^-	Cluster size	
	Magic number	First hydrated shell
HO^-	10, 12, 14	3
O_2^-	3, 13, 15	4
HO_2^-	6, 9, 20	–
NO_2^-	8	–
CO_3^-	10,16	2
NO_3^-	9,15	2
HCO_4^-	10,16	3
$NO_3^-(HNO_3)_2$	8	–

of $O^-(H_2O)_n$, $O_2^-(H_2O)_n$ and $O_3^-(H_2O)_n$ (n = 0–4), focusing on the binding energy between the anion and the water [28]. They demonstrated that the $O_2^-(H_2O)_4$ having a C_i symmetry corresponds to the first hydrated shell in the $O_2^-(H_2O)_n$ cluster series. According to the experimental and theoretical results obtained by Weber et al. and Seta et al., in contrast, the $O_2^-(H_2O)_3$ are most likely to retain dimeric core structure of $O_2^-(H_2O)_2$ having C_{2h} and/or C_1 symmetries with the third H_2O molecule attached to the ion in a remote binding site [26–28]. These results suggest that the $O_2^-(H_2O)_3$ is unstable compared to $O_2^-(H_2O)_4$ and $O_2^-(H_2O)_2$, which is inconsistent with the result obtained here. Our mass spectrometry data clearly exhibits the specific stability of $O_2^-(H_2O)_3$ as a magic number. Further progress in understanding the origin of the stability of $O_2^-(H_2O)_3$ observed here will require experimental and theoretical studies.

4. Conclusions

Here we report the influence of orifice temperature on the size distribution in water clusters $Y^-(H_2O)_n$ with various negative atmospheric core ions Y^- such as O_2^-, HO^-, HO_2^-, NO_2^-, NO_3^-, $NO_3^-(HNO_3)_2$, CO_3^- and HCO_4^-, using atmospheric pressure DC negative corona discharge mass spectrometry. The cluster distributions with high peak intensity were shifted to smaller cluster size with increasing orifice temperature. This was caused by the inhibition of large water cluster formation due to insufficient cooling during adiabatic expansion in the vacuum region of the mass spectrometers. In contrast, the reproducible anomalous discontinuities in ion peak intensity at certain size clusters $Y^-(H_2O)_m$ in the $Y^-(H_2O)_n$ cluster series observed at the lowest orifice temperature, which has been recently reported [18], did not vary with change in temperature. These results suggested that the clusters $Y^-(H_2O)_m$ are more stable than other size clusters $Y^-(H_2O)_n$, independent of thermochemical conditions. Thus, the $Y^-(H_2O)_m$ correspond to the magic number or first hydrated shell in the cluster series $Y^-(H_2O)_n$. The particular stability of $Y^-(H_2O)_m$ was also confirmed by using the ratio of the $Y^-(H_2O)_n$ to $Y^-(H_2O)_{n+1}$ peak intensity, which was proposed by Zhang et al. as a reliable method for identifying the magic numbers in arbitrary cluster distributions obtained by varying the temperature and solvent partial pressure in a reaction chamber [8]. An interesting result obtained here was the finding that the specific high stability of $O_2^-(H_2O)_3$ and $O_2^-(H_2O)_4$ as the magic number and first hydrated shell in the $O_2^-(H_2O)_n$ cluster series, respectively. The observation of the first hydrated shell $O_2^-(H_2O)_4$ is in good agreement with the previous studies using infrared spectroscopy and *ab initio* calculations [26–28], while those previous studies have described the instability of $O_2^-(H_2O)_3$, which is inconsistent with the result obtained here. Further experimental and theoretical studies regarding the stability of $O_2^-(H_2O)_3$ will be required.

Acknowledgements

This work was supported by Research Fellowships of the Japan Society for the Promotion of Science for Young Scientists granted under No. 20.10498.

References

[1] F. Yu, R.P. Turco, Geophys. Res. Lett. 27 (2000) 883.
[2] H.D. Beckey, Z. Naturforsch. 14 (1959) 712.
[3] H.D. Beckey, Z. Naturforsch. 15 (1960) 822.
[4] S.S. Lin, Rev. Sci. Instrum. 44 (1973) 516.
[5] J.Q. Searcy, J.B. Fenn, J. Chem. Phys. 61 (1974) 5282.
[6] M. Tsuchiya, T. Tashiro, A. Shigahara, J. Mass Spectrom. Soc. Jpn. 52 (2004) 1.
[7] G. Schlosser, Z. Takáts, K. Vékey, J. Mass Spectrom. 38 (2003) 1245.
[8] X. Zhang, A.W. Castleman Jr., J. Chem. Phys. 101 (1994) 1157.
[9] S. König, H.M. Fales, J. Am. Soc. Mass Spectrom. 9 (1998) 814.
[10] H. Haberland, in: J. Eichler, I.V. Hertel, N. Stolterfoht (Eds.), Electric and Atomic Collisions, Elsevier, Amsterdam, 1984, p. 597.
[11] U. Nagashima, S. Shinohara, N. Nishi, H. Tanaka, J. Chem. Phys. 84 (1986) 209.
[12] A.J. Cunningham, J.D. Payzant, P. Kebarle, J. Am. Chem. Soc. 94 (1972) 7627.
[13] Y.K. Lau, S. Ikuta, P. Kebarle, J. Am. Chem. Soc. 94 (1982) 1462.
[14] M. Meot-Ner, C.V. Speller, J. Phys. Chem. 90 (1986) 6616.
[15] J.M. Kassner Jr., D.E. Hagen, J. Chem. Phys. 64 (1976) 1860.
[16] F.C. Pickard, E.K. Pokon,.D. Liptak, G.C. Shields, J. Chem. Phys. 122 (2005) 024302.
[17] M. Eigen, Angew. Chem. Int. Ed. 3 (1964) 1.
[18] K. Sekimoto, M. Takayama, J. Mass Spectrom. 45 (2010) 50.
[19] K. Sekimoto, M. Takayama, Int. J. Mass Spectrom. 261 (2007) 38.
[20] K. Sekimoto, M. Takayama, Eur. Phys. J. D 50 (2008) 297.
[21] K. Sekimoto, M. Takayama, Eur. Phys. J. D 60 (2010) 589.
[22] X. Yang, A.W. Castleman Jr., J. Am. Chem. Soc. 111 (1989) 6845.
[23] M. Arshadi, P. Kebarle, J. Phys. Chem. 74 (1970) 1583.
[24] W.H. Robertson, E.G. Diken, E.A. Price, J.-W. Shin, M.A. Johnson, Science 299 (2003) 1367.
[25] M.D. Newton, S. Ehrenson, J. Am. Chem. Soc. 93 (1971) 4971.
[26] J.M. Weber, J.A. Kelley, S.B. Nielsen, P. Ayotte, M.A. Johnson, Science 287 (2000) 2461.
[27] J.M. Weber, J.A. Kelly, W.H. Robertson, M.A. Johnson, J. Chem. Phys. 114 (2001) 2698.
[28] T. Seta, M. Yamamoto, M. Nishioka, M. Sadakata, J. Chem. Phys. 107 (2003) 962.